Available online at www.sciencedirect.com
SCIENCE DIRECT®
Journal of the European Ceramic Society 25 (2005) 447–454
www.elsevier.com/locate/jeurceramsoc

# Direct observation of ferroelastic domain switching in polycrystalline $BaTiO_3$ using in situ neutron diffraction

J. S. Forrester [a,*], E. H. Kisi [a], A. J. Studer [b]

[a] *School of Engineering, University of Newcastle, Callaghan, NSW 2308, Australia*
[b] *Bragg Institute, Australian Nuclear Science and Technology Organisation, PMB 1, Menai, NSW 2234, Australia*

Received 24 October 2003; received in revised form 9 March 2004; accepted 21 March 2004
Available online 21 July 2004

**Abstract**

The extent and nature of ferroelastic re-orientation in a $BaTiO_3$ ceramic under compressive stresses up to 150 MPa were studied using strain gauges and in-situ neutron powder diffraction. At ≥10 MPa during the first loading, the unpoled crystals shows ferroelastic re-orientation. By 80 MPa ∼12% of the material oriented for diffraction has switched. Nearly half of the switched material reverts to its original orientation upon relaxation of the load, leaving 7% permanently switched. Successive load cycles have little further effect. It is unlikely that the ferroelasticity observed here makes a significant contribution to toughening as it saturates at relatively low stresses, such as exist only in the outer region of the process zone.


*Keywords:* $BaTiO_3$; Ferroelectric properties; Ferroelastic domain switching; Domains; Neutron diffraction

## 1. Introduction

Ferroelectric ceramics are generally optimised for maximum piezoelectric effect; however, they are known to have poor mechanical properties. There has been recent interest in both static and cyclic load-bearing applications for ferroelectric materials.[1,2] A major hindrance in extending ferroelectric materials to two markets, namely multilayer actuators in fuel injection systems and ferroelectric memories, is their limited lifetime.[3]

While the geometrical problems of field and stress singularities have been overcome somewhat, reliability remains an issue at high cycle numbers in cyclic loading applications. Tai and Kim[2] examined various $Pb(Zr_xTi_{1-x})O_3$ (PZT) compositions with respect to their degradation with repeated cycling of compressive load, with indications that in unpoled samples the internal stresses are isotropic, while in the poled samples the stresses are anisotropic. Owing to the poling treatment, a compressive and tensile stress occurred parallel and perpendicular to the poling direction. $k_{33}$ decreased linearly with cyclic loading in morphotropic phase boundary and rhombohedral compositions. The decrease in $k_{33}$ was slow in the tetragonal composition until 5% of the fatigue life, suggesting that the tetragonal structure performed better under these cyclic conditions.

An additional complication is internal microstresses, which are detrimental to the strength of ceramics. Early work by Pohanka et al.[4] examined internal stresses caused by the transition from the paraelectric cubic to the ferroelectric tetragonal phase in $BaTiO_3$. A range of doped and undoped samples, and samples stabilised in the cubic phase using LiF and MgO, were used to demonstrate that internal stresses caused by the phase transition add to any applied stress, thereby weakening the material. Doped $BaTiO_3$ did not change significantly in strength above and below the $T_C$. A TEM study of $BaTiO_3$ revealed that the strain generated during the transition is taken up inhomogeneously along and across the domain boundaries, and these local strains weaken the material.[5]

The non-linear mechanical response of ferroelectrics is well-documented, and there is a considerable body of evidence that this is due to ferroelasticity or mechanically instigated domain re-orientation.[6–8] Ferroelasticity is of great interest because it may contribute to the fracture toughness in some ceramics,[9,10] including ferroelectrics.[11] Crystallographic domains spontaneously re-align to produce

* Corresponding author. Tel.: +61-2-4921-6117; fax: +61-2-4921-7050.
*E-mail address:* jforrest@mail.newcastle.edu.au (J.S. Forrester).

0955-2219/$ – see front matter © 2004 Elsevier Ltd. All rights reserved.
doi:10.1016/j.jeurceramsoc.2004.03.018

permanent deformation, resulting in hysteresis in the stress–strain curve, and a mechanism for mechanical poling. It is not yet certain if the ferroelasticity that occurs in ferroelectric ceramics significantly influences the fracture toughness.

In the proposed ferroelastic toughening mechanism, the domains re-orient allowing the ceramic to absorb energy stored in the highly strained area around a crack tip. Indentation-induced cracking on particular orientations of $BaTiO_3$ single crystals has shown that most indentation angles favour switching of 90° domains.[12,13] Förderreuther et al.[14] have observed *R*-curve behaviour in $BaTiO_3$ ceramics and attributed it to mechanisms such as ferroelasticity. Meschke et al.[15] used an atomic force microscope tip to measure crack opening displacement, with the conclusion that the fracture toughness of $BaTiO_3$ is increased by 50% by ferroelastic domain switching, which is therefore a major toughening mechanism. In contrast, using theoretical arguments Reece and Guiu[6] have estimated only a 10% contribution to fracture toughness, concluding that ferroelasticity cannot be as significant as say, phase transformations in zirconia ceramics.

To establish the contribution of ferroelastic domain switching in ferroelectric ceramics to toughening, the basic characteristics of the ferroelasticity need to be established. A direct crystallographically sensitive method of measurement is necessary. Diffraction data collected in-situ (i.e. simultaneous to an applied load) provide real-time results free from relaxation effects. Neutron diffraction (ND) is particularly appropriate because domain switching is largely accomplished by re-orientation of the oxygen ions which scatter neutrons strongly, and also because neutron diffraction patterns represent the entire sample rather than the near surface region. This study examines the mechanical behaviour of $BaTiO_3$, focusing on the role of internal strains and ferroelasticity in toughening under stress, and unequivocally demonstrates the occurrence of ferroelastic domain re-orientation. The effectiveness of ferroelastic domain switching as a toughening mechanism is discussed, along with the impact that increased internal strains due to domain switching have on the mechanical properties of the ceramic.

## 2. Experimental

Polycrystalline $BaTiO_3$ pieces were purchased from the Aldrich Chemical Company.[1] X-ray diffraction (XRD) patterns were collected from several samples to verify phase purity. All major reflections indexed as tetragonal. An examination of the background intensity revealed little anomalous intensity, and it was inferred that little, if any, second phase was present. The microstructure is shown in Fig. 1 to contain large tabular crystals separated by regions of residual porosity. For the in-situ neutron diffraction it was important to maximise counting statistics and so two pieces

[1] P.O. Box 355 Milwaukee, WI 53233, USA.

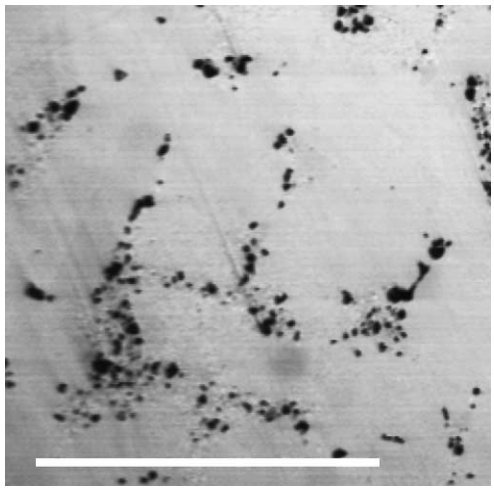

Fig. 1. Reflected light laser scanning confocal microscope image showing the microstructure of the $BaTiO_3$ samples. The scale marker is 100 μm.

with the same lateral dimensions were stacked. The samples were ground and stacked to make a rectangular prism with dimensions of 8 mm × 10 mm × 12.45 mm (996 $mm^3$).

A 200 kN loading device designed to fit on the specimen stage of the medium resolution powder diffractometer (MRPD) at the Australian Nuclear Science and Technology Organisation (ANSTO) was used to apply mechanical loads to samples.[10] All tests were conducted under similar conditions, with the steel testing machine short circuiting the sample. Loads were applied vertically, with the neutron diffraction pattern recorded in the horizontal plane. Macroscopic strains were measured using strain gauges glued transversely and longitudinally on all vertical faces of the sample. Strain gauge data were recorded every 30 s for the duration of the experiments.

Prior to the in-situ experiment similar samples of $BaTiO_3$ were loaded to estimate the compressive strength. The sample remained intact at 200 MPa of stress, but visual inspection showed small pieces had broken away, indicating imminent fracture. A maximum stress of 150 MPa was used during the neutron diffraction experiments, as it was desirable that the samples remained intact so data could be collected during unloading and reloading. Each sample was loaded in 10 MPa steps to 150 MPa, and then unloaded in 30 MPa steps to zero. Reloading occurred in 30 MPa steps to 150 MPa, and returned to zero in the same way. ND patterns were collected simultaneously over the $2\theta$ range 2–129° in 0.1° steps. The steps were timed by 48,000 counts in a low efficiency primary beam monitor.

## 3. Results and discussion

### 3.1. Stress–strain results

Stress–strain results derived from a transverse and a longitudinal gauge are shown in Fig. 2. These data were obtained by taking a single point toward the end of each

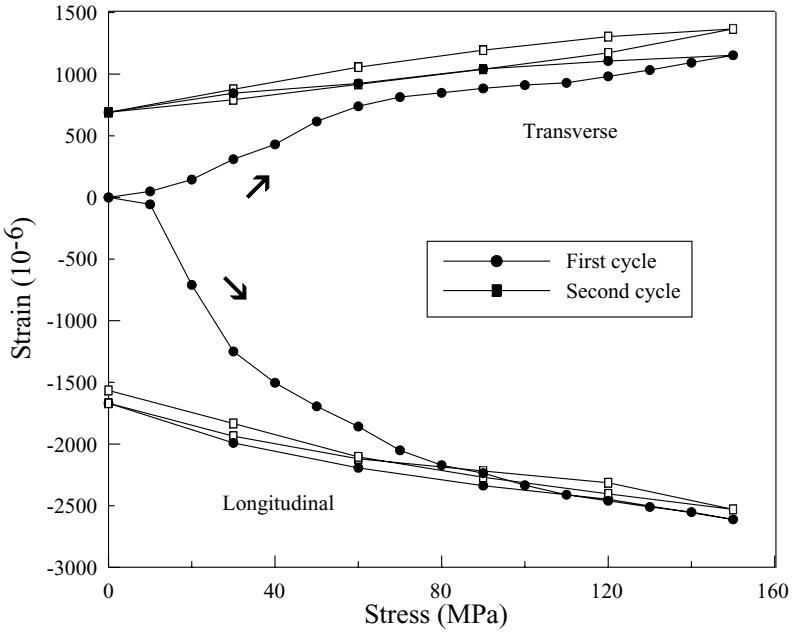


Fig. 2. Stress–strain curves derived from the end-points of each constant stress hold in the strain-time data. The curve is non-linear until 80 MPa and linear thereafter.

incremented step and plotting it as a function of the applied stress at that step. Major deformation clearly occurs in the sample in the initial steps of the first loading. Strain during the initial step is relatively small and appears to be approximately 100% elastic. The strain during the next few load increments is much larger. There is a strong resemblance between these data and those of similar tests on PZT.[8] Above 80 MPa, the increased stress primarily resulted in elastic strain in the sample. The strain increments then become smaller until the maximum load. Upon stepping down, the strain does not return to zero, with the longitudinal strain finishing at approximately $1700 \times 10^{-6}$, and the transverse strain at approximately $700 \times 10^{-6}$. The reload data are similar in appearance to the unload data, especially for the longitudinal strain gauge. There is evidence of some reproducible non-linearity especially by comparing strains during the first and second unload with the reload data in the longitudinal gauge.

### 3.2. Neutron diffraction patterns

Neutron diffraction patterns collected simultaneously to the applied stress show the effect on diffraction peaks, and several selected patterns are shown in Fig. 3. Patterns are shown prior to loading (0 MPa (1)), at 30, 50 and 150 MPa of the first stress cycle, after the sample was fully stepped down (0 MPa (2)), after the sample was fully re-loaded (150 MPa), and after completion of the two loading cycles (0 MPa (3)). Major tetragonal reflections are marked on the 0 MPa pattern. Two minor reflections, at 48° $2\theta$ and 64° $2\theta$, were identified as not belonging to $BaTiO_3$ and were not visible in the XRD patterns. During the experiment, components of the loading device were masked using cadmium foil, however, the extra reflections are due to minor scattering from the load frame above and below the masking.

Intensities and widths of many reflections (e.g. (1 1 1)) did not alter significantly during the loading and unloading cycles. The most significant changes occurred in twin-related reflections, such as the (0 0 2)/(0 2 0) pair at approximately 48.9 and 49.3° $2\theta$, and are most easily observed in the (1 1 3)/(1 3 1) pair at approximately 86.8 and 87.5° $2\theta$. These reflections are enlarged in the insets in Fig. 3. Initially in the (1 1 3)/(1 3 1) doublet, the (1 1 3) reflection height is about half that of the (1 3 1) reflection.[2] With applied stress the intensity of the (1 1 3) reflection increases, with a corresponding intensity decrease in (1 3 1). Above 70 MPa, the reflections approach equal height. With the load removed the trend reverses itself, but does not resume the original ratio. The second loading cycle is qualitatively similar to the first. The trends in the (0 0 2) and (0 2 0) reflections are similar but not so pronounced because of reflection overlap. At 0 and 30 MPa, the (0 0 2) reflection is weaker than the (0 2 0), at 50 MPa it becomes greater than the (0 2 0), and at 150 MPa it appears significantly larger. On unloading, the (0 2 0) and (0 0 2) intensities became approximately equal. All of these changes in relative intensities are attributable to ferroelastic domain switching.

### 3.3. Rietveld refinement

Whole pattern analyses were conducted using the Rietveld refinement program LHPM[16], and the refinements followed

[2] This reflection also includes the (3 1 1) reflection, but tetragonal symmetry constrains these reflections to identical positions.

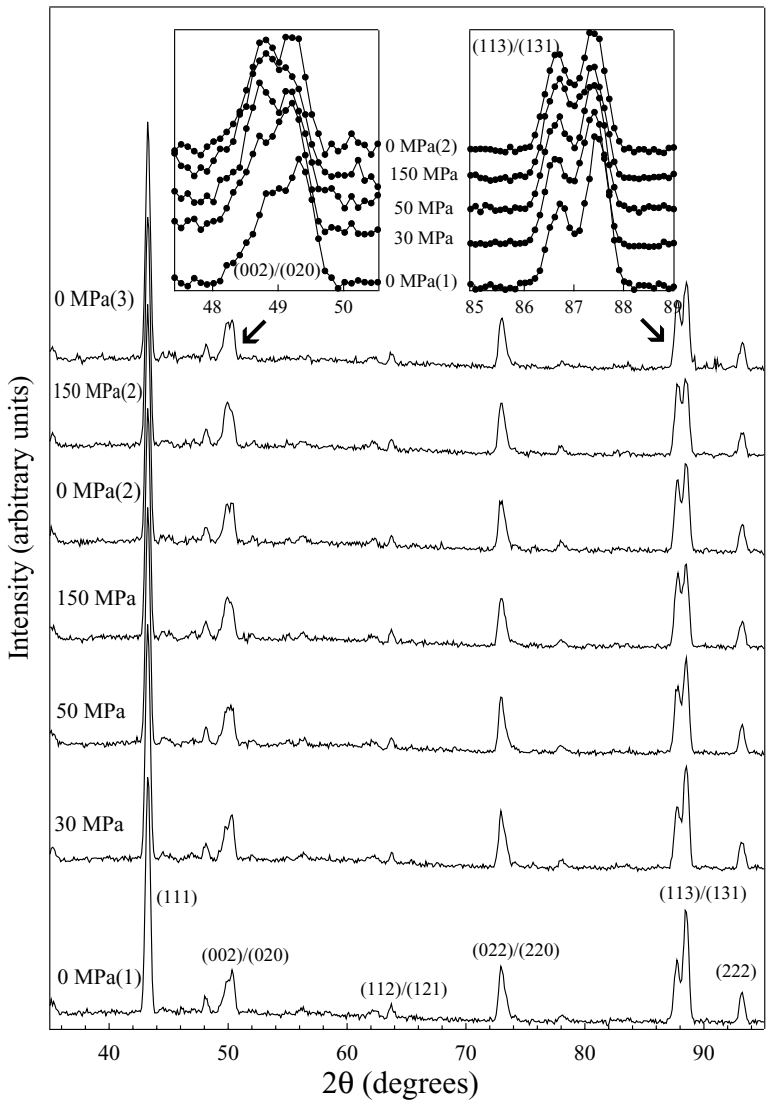


Fig. 3. Neutron diffraction patterns collected during a loading cycle in $BaTiO_3$. Several patterns are shown during the first loading cycle, followed by fully unloaded, fully reloaded, and fully unloaded again. *Insets*: The (0 0 2)/(0 2 0) and (1 1 3)/(1 3 1) reflections enlarged and vertically offset to show changes in relative reflection intensities during loading and unloading. There is transfer of intensity to the (0 0 2) and (1 1 3) reflections up to 150 MPa indicating domain re-orientation.

the procedure outlined by Young[17]. The loading device partially blocked the detectors and so the Rietveld refinement $2\theta$ range was restricted to 20–100°. Several instrumental reflection width and shape parameters were fixed. The asymmetry parameter was set at 0.05, the Gaussian full-width at half-maximum (FWHM) parameters $V$ at $-0.23$ and $W$ at 0.26, and the Lorentzian FWHM, $K$ at 0.002. The thermal parameters were refined to be $B_{Ba} = 0.45\,Å^2$, $B_{Ti} = 0.34\,Å^2$, $B_{O1} = 1.11$ and $B_{O2} = 0.94\,Å^2$ from a diffraction pattern collected prior to loading. These were used as the starting values in subsequent refinements. The parameters refined in all patterns were the scale factor ($s$), third order polynomial background coefficients, zero point offset, the lattice parameters ($a$ and $c$), the atomic co-ordinates, the width parameter ($U$), the full width of the Lorentzian component of the Voigt peak shape function ($k$) and the preferred orientation coefficient, $r$ (using the March–Dollase model). Typically the refinements achieved $R_{wp}$ values of better than 8%, and $R_p$ values better than 6%. The Bragg $R$ ($R_B$) factors are considerably smaller and are presented in Table 1.

Examples of Rietveld refinement plots are shown in Fig. 4, at 0 and 150 MPa. The crosses represent experimental data, the continuous line through them is the calculated pattern, the line below is the difference between the experimental and calculated pattern, and the markers beneath indicate the allowed ($h\,k\,l$) for tetragonal $BaTiO_3$. Refined values of $U$, $r$, $a$ and $c$ for the series of diffraction patterns are presented in Table 1.

Trends in the March coefficient are shown in Fig. 5. Prior to loading, the March coefficient was 0.94(1), indicating a small amount of pre-existing preferred orientation. This may have resulted from processing (such as hot-pressing),

Table 1
Refined Rietveld parameters for $BaTiO_3$

| Stress (MPa) | Gaussian FWHM ($U$) | March coefficient ($r$) | Unit cell ($a$) | Unit cell ($c$) | $R_B$ (%) |
|---|---|---|---|---|---|
| 0 | 0.25(2) | 0.94(1) | 3.9958(4) | 4.0352(5) | 1.33 |
| 10 | 0.27(2) | 0.93(1) | 3.9960(5) | 4.0351(7) | 1.63 |
| 20 | 0.28(2) | 0.913(9) | 3.9951(4) | 4.0334(5) | 1.05 |
| 30 | 0.28(1) | 0.912(9) | 3.9948(4) | 4.0327(5) | 0.96 |
| 40 | 0.27(1) | 0.888(9) | 3.9955(4) | 4.0342(5) | 0.96 |
| 50 | 0.28(1) | 0.863(9) | 3.9951(4) | 4.0332(5) | 1.10 |
| 60 | 0.28(1) | 0.867(9) | 3.9957(4) | 4.0333(5) | 1.02 |
| 70 | 0.28(1) | 0.868(9) | 3.9957(4) | 4.0331(5) | 1.30 |
| 80 | 0.29(1) | 0.844(9) | 3.9950(4) | 4.0323(5) | 1.22 |
| 90 | 0.31(1) | 0.841(9) | 3.9950(4) | 4.0324(5) | 1.12 |
| 100 | 0.30(1) | 0.837(8) | 3.9958(4) | 4.0328(5) | 1.29 |
| 110 | 0.30(1) | 0.837(9) | 3.9962(4) | 4.0333(5) | 1.59 |
| 120 | 0.29(1) | 0.831(8) | 3.9956(4) | 4.0329(5) | 1.50 |
| 130 | 0.31(1) | 0.825(8) | 3.9952(4) | 4.0327(5) | 1.54 |
| 140 | 0.32(1) | 0.819(8) | 3.9963(5) | 4.0329(5) | 1.63 |
| 150 | 0.30(1) | 0.827(9) | 3.9958(5) | 4.0322(5) | 1.73 |
| 120 | 0.30(1) | 0.829(8) | 3.9954(4) | 4.0323(5) | 1.39 |
| 90 | 0.30(1) | 0.846(9) | 3.9947(4) | 4.0325(5) | 1.06 |
| 60 | 0.29(1) | 0.867(8) | 3.9948(4) | 4.0330(5) | 1.26 |
| 30 | 0.28(1) | 0.862(8) | 3.9942(4) | 4.0324(5) | 1.51 |
| 0 | 0.28(1) | 0.856(8) | 3.9950(4) | 4.0329(5) | 1.35 |
| 30 | 0.28(1) | 0.853(9) | 3.9948(4) | 4.0330(5) | 1.51 |
| 60 | 0.29(1) | 0.846(8) | 3.9952(4) | 4.0330(4) | 1.48 |
| 90 | 0.31(1) | 0.828(8) | 3.9954(4) | 4.0326(5) | 1.77 |
| 120 | 0.31(1) | 0.821(9) | 3.9958(5) | 4.0326(5) | 1.49 |
| 150 | 0.30(1) | 0.816(8) | 3.9953(5) | 4.0317(5) | 1.15 |
| 120 | 0.30(1) | 0.834(9) | 3.9952(4) | 4.0322(5) | 1.55 |
| 90 | 0.31(1) | 0.835(8) | 3.9953(4) | 4.0326(5) | 1.18 |
| 60 | 0.29(1) | 0.853(9) | 3.9969(4) | 4.0348(4) | 1.47 |
| 30 | 0.27(1) | 0.859(8) | 3.9968(4) | 4.0347(5) | 1.22 |
| 0 | 0.27(1) | 0.863(9) | 3.9947(5) | 4.0328(5) | 1.16 |

or domain re-orientation upon cooling through the Curie temperature. There is a decrease in the March coefficient from 0.94(1) to 0.865(9) during the initial 50 MPa of stress due to ferroelastic domain re-orientation. Thereafter it follows a similar path to the macroscopic strains in Fig. 2.

The Gaussian half-width parameter $U$ is often associated with the degree of intercrystalline strain in a sample. Here, $U$ increased from 0.28(2) to 0.36(2) during loading, and decreased with unloading, however, not reaching its initial value. This indicates that ferroelastic switching has increased the level of internal or residual strain, which may be detrimental to mechanical properties.

The refined lattice parameters $a$ and $c$ showed only minor changes. The range in lattice parameter $a$ is 0.0021 and for the $c$ is 0.0028. There is a notable contraction of the $c$-axis in the initial few steps of loading, but apart from this, little else warrants comment. Other refined parameters showed little systematic variation. The only atomic co-ordinates refinable were the $z$ co-ordinates of titanium and two oxygen ions, and the values are included in Table 1. The $R_B$ values for the series of refinements lie between 0.93 and 3.06. There are strong trends in $R_B$, $R_p$ and $R_{wp}$ values, with the $R_B$ values chosen to demonstrate them included in Table 1. The trends are possibly due to elastic anisotropy,[10] but the data are not sufficiently precise to be used to determine single crystal elastic constants by the procedure of Kisi and Howard.[18]

### 3.4. Integrated intensity analyses

To quantify the degree of ferroelasticity, the reflection doublets (0 0 2)/(0 2 0) comprising crystals oriented at 90° to each other and (1 1 3)/(1 3 1) reflections oriented at 84.78 and 95.22° to each other were analysed. The integrated intensities for the first stress cycle were extracted using the programs EXCEL and PEAKFIT. The (1 1 3) and (1 3 1) reflections were well-separated, and easily fitted with two Gaussian curves as shown in Fig. 6. The (0 0 2)/(0 2 0) pair were not so well-separated (Fig. 3 inset). In addition, significant asymmetry on the lower $2\theta$ side of the (0 0 2)/(0 2 0) reflections made fitting more difficult. However, for consistency the same strategy was adopted. In each case, the FWHM was restrained to be the same for each twin-related reflection.

An example of relative intensity changes is shown in Fig. 7 for the (1 1 3)/(1 3 1) reflections refined using EXCEL. Similar results were obtained using PEAKFIT. Several trends are observable. First, the total intensity, shown at the top of the figure, remains constant with applied stress, i.e. the increase in intensity of the (1 1 3) reflection mirrors the decrease in

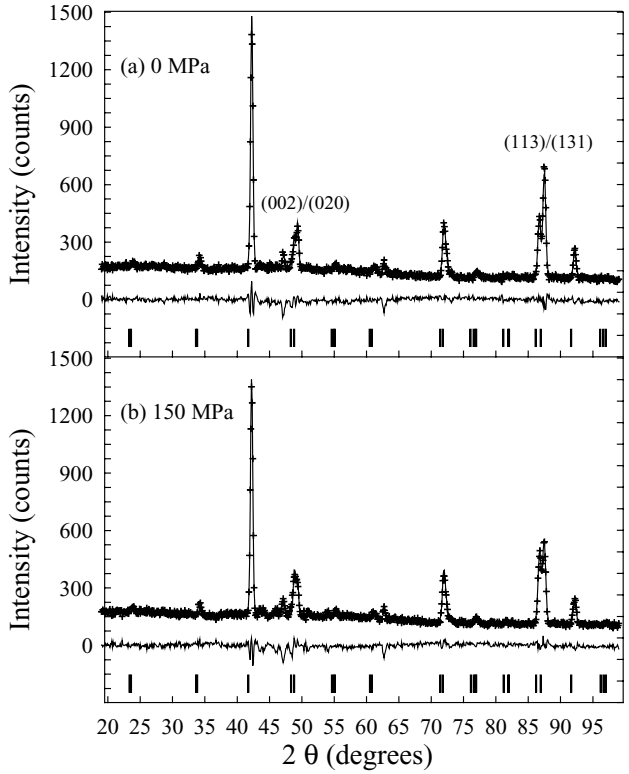


Fig. 4. Rietveld refinements of $BaTiO_3$ sample (a) prior to an applied stress: (0 MPa); and (b) at the maximum stress: (150 MPa). The background in MRPD with the loading device in place is irregular, but still able to be modelled. The minor reflections attributed to the loading device can be seen at 48° 2$\theta$ and 64° 2$\theta$. The difference pattern indicates an acceptable fit between the calculated pattern and the experimental data.

intensity of (1 3 1). Intensities are similar at 100 MPa, and there is little further change with further increase in stress. Second, during unloading the intensities revert to their previous values until approximately 40 MPa, and then deviate from the loading data thereafter. Intensity changes in the (0 0 2)/(0 2 0) reflections show similar features although there is a greater scatter among the results. Third, after the loading/unloading, more intensity remains in the (0 0 2) and (1 1 3) reflections, and less in the (0 2 0) and (1 3 1) reflections. This is an indication of the proportion of domains that have permanently switched during the loading process.

Fig. 8 shows that there is an increase in the (1 1 3)/(1 3 1) FWHM with applied stress, and a decrease with a decreasing stress. The (0 0 2)/(0 2 0) doublet shows a similar trend but with greater scatter. These FWHM changes indicate interdomain and intercrystalline stresses, some of which remain on unloading.

### 3.5. Ferroelastic domain quantification

Using the method of Ma et al.[19] the integrated intensities calculated above were used to estimate the proportion of domains undergoing domain switching as a function of stress. The method was applied to both the (1 1 3)/(1 3 1) and (0 0 2)/(0 2 0) reflections, and the former results are presented. The proportion of unit cells with their (1 1 3) planes normal to the applied stress is presented in Fig. 9. Up to 40 MPa a significant proportion of domains are so oriented, from approximately 38 to 45%. Thereafter the switching continues in a regular fashion to a maximum of about 51% at the maximum stress. With the removal of the load, those domains that have switched at the stresses above 40 MPa revert to their former orientations. However, the domains that switched below 40 MPa do not appear to have relaxed to their former positions. The similarities between these data and those shown in the strain gauge results in Fig. 2 are obvious. Strains remain higher after unloading, which relates to the permanent switching of domains shown in Fig. 9. The values in Fig. 9 were converted into total domains re-oriented with applied load, and these follow the same pattern. At the maximum load, over 12% of the domains are re-oriented, but when the load is decreased this value reduces to 7%. From this figure, it can be estimated that 5% of domains are reversibly switched, and 7% that switched orientation during the early stages of loading, were irreversibly switched.

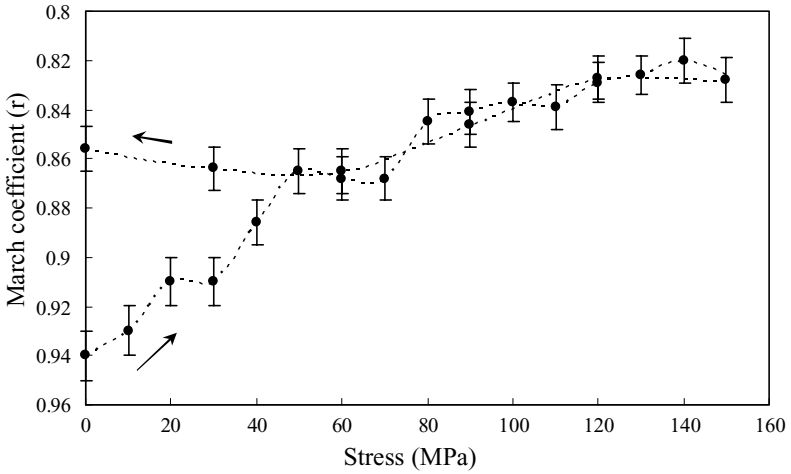


Fig. 5. Preferred orientation of crystallites as indicated by the March coefficient.

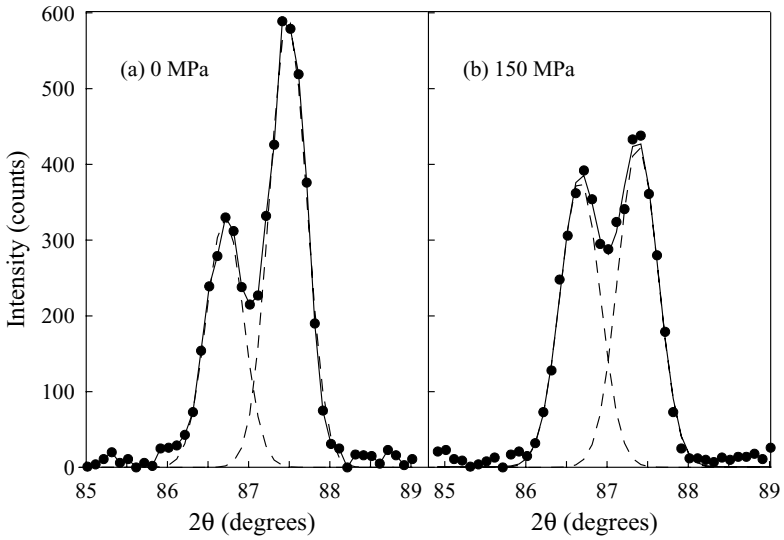


Fig. 6. Examples of peak-fitting analyses using Gaussian functions to model the (1 1 3) and (1 3 1) reflections: (a) with no applied stress and (b) at 150 MPa.

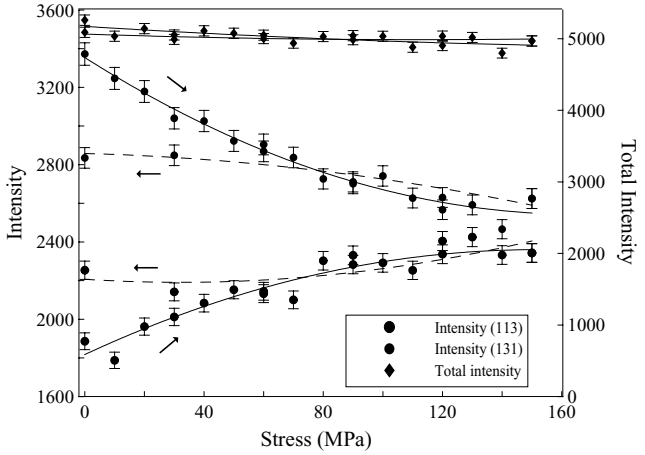


Fig. 7. Changes in intensity with increasing load in the (1 1 3)/(1 3 1) reflections refined using the program EXCEL. The total refined intensity is shown above referenced to the right hand *y*-axis. The lines are added to guide the eye.

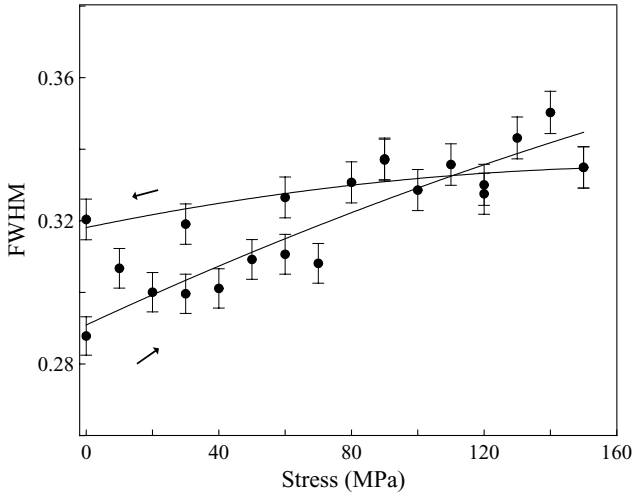


Fig. 8. The refined FWHMs for the (1 1 3)/(1 3 1) reflections.

### *3.6. Ferroelasticity as a toughening mechanism in $BaTiO_3$*

Mechanisms leading to *R*-curve behaviour operate from some critical stress up to the fracture stress. That is, the microstructural toughening mechanism adds dynamic range to the upper end of the fracture resistance. In contrast, in these samples, the observed saturation of ferroelasticity at 80 MPa is well below the fracture stress of >200 MPa. Therefore, a majority of the switchable domains for the prevailing stress conditions have already switched well before fracture. This suggests that ferroelasticity is not a major toughening mechanism in this ceramic.

Similar conclusions may be drawn from a consideration of the stress distribution, as a function of distance *l* from the crack tip, in the unperturbed process zone ahead of a sharp

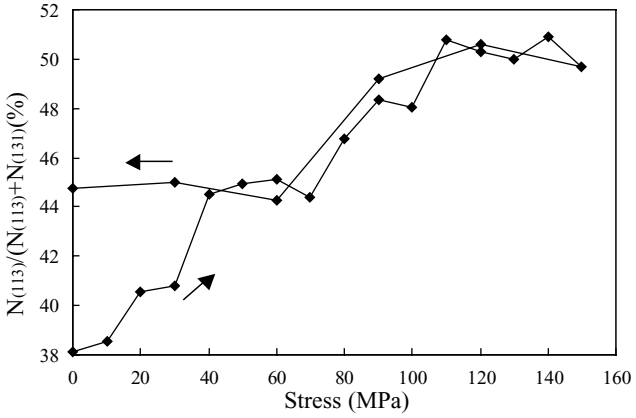


Fig. 9. The proportion of crystallites with (1 1 3) planes normal to the scattering vector with increased static loads.

mode I crack which can be approximated by

$$\sigma = \sigma_{av} + \sigma_{av}\sqrt{\frac{a}{2l}} \quad (1)$$

where $\sigma_{av}$ is the average or nominal stress and $a$ is the crack depth. At any stress approaching the saturation stress, ferroelasticity is only active within that part of the process zone most remote from the crack tip. At nominal stresses greater than 80 MPa, no ferroelasticity is expected within the process zone unless the crack orientation is at odds with the orientation of the externally applied stress.

These results appear to contradict the results of Meschke et al.[15] using compact tension specimens and monitoring the near-crack region with atomic force microscopy. It is possible that the difference arises in the different loading types, or perhaps in microstructural differences, their sample having equiaxed grains in the range 0.5–5 μm and our tabular grains approximately 100 μm long. The results also differ from the X-ray diffraction results on hard PZT samples by Glazounov et al.[20,21] however, their material has a coercive stress of ∼55 MPa compared with ∼10 MPa in the soft $BaTiO_3$ studied here.

## 4. Conclusions

The results presented here indicate that, in the particular ceramic studied, ferroelastic domain switching may not be a useful toughening mechanism because it occurs at low stresses (less than 80 MPa), and is therefore, saturated in the near-crack region of the process zone. In addition, the internal strains that occur as a result of the domain switching may detrimentally affect the toughness.

Several conclusions may be reached from this experimental work. These include:

1. Ferroelasticity has a role in the mechanical deformation in the initial loading of $BaTiO_3$ ceramics at low stresses.
2. In-situ neutron diffraction illuminates this role by allowing the direct observation of reflection intensity changes of twin-related reflections due to domain re-orientation.
3. Analysis of diffraction reflection data can provide an approximation of the percent of domains that switch during load changes.
4. In this experiment, the amount of domains switched under maximum load is 12%. Of this 12%, 5% switch back when the load is removed and 7% remain in their new orientation.

## Acknowledgements

The authors thank the Australian Research Council and the Australian Institute of Nuclear Science and Engineering for providing financial support for the experimental work.

## References

1. Zhang, Z. and Raj, R., Influence of grain size on ferroelastic toughening and piezoelectric behaviour of lead zirconate titanate. *J. Am. Ceram. Soc.* 1995, **78**, 3363–3368.
2. Tai, W.-P. and Kim, S.-H., Relationship between cyclic loading and degradation of piezoelectric properties in $Pb(Zr,Ti)O_3$ ceramics. *Mater. Sci. Eng. B* 1996, **38**, 182–185.
3. Wang, Q.-M. and Cross, L. E., Tip deflection and blocking force of soft PZT-based cantilever RAINBOW actuators. *J. Am. Ceram. Soc.* 1999, **82**, 103–110.
4. Pohanka, R. C., Rice, R. W. and Walker, Jr. B.E., Effect of internal stress on the strength of $BaTiO_3$. *J. Am. Ceram. Soc.* 1976, **59**, 71–74.
5. Chou, J.-F., Lin, M.-H. and Lu, H.-L., Ferroelectric domains in pressureless-sintered barium titanate. *Acta Mater.* 2000, **48**, 3569–3579.
6. Reece, M. J. and Guiu, F., Estimation of the toughening produced by ferroelectric/ferroelastic domain switching. *J. Eur. Ceram. Soc.* 2001, **21**, 1433–1466.
7. Fett, T. and Munz, D., Measurement of Young's moduli for lead zirconate titanate (PZT) ceramics. *J. Test. Eval.* 2000, **28**, 27–35.
8. Forrester, J. S. and Kisi, E. H., Ferroelastic switching in a soft lead zirconate titanate. *J. Eur. Ceram. Soc.* 2004, **24**(3), 595–602.
9. Virkar, A. V. and Matsumoto, R. L. K., Ferroelastic domain switching as a toughening mechanism in tetragonal zirconia. *J. Am. Ceram. Soc.* 1986, **69**, 224–226.
10. Kisi, E. H., Kennedy, S. J. and Howard, C. J., Neutron diffraction observations of ferroelastic domain switching and tetragonal-to-monoclinic transformation in Ce-TZP. *J. Am. Ceram. Soc.* 1997, **80**, 621–628.
11. Garg, A. and Goel, T. C., Mechanical and electrical properties of PZT ceramics (Zr:Ti = 0.40:0.60) related to $Nd^{3+}$ addition. *Mater. Sci. Eng. B: Solid State Mater. Adv. Technol.* 1999, **60**(2), 128–132.
12. Fang, F. and Yang, W., Indentation-induced cracking and 90° domain switching pattern in barium titanate ferroelectric single crystals under different poling. *Mater. Lett.* 2002, **57**, 198–202.
13. Munoz-Saldana, J., Schneider, G. A. and Eng, L. M., Stress induced movement of ferroelastic domain walls in $BaTiO_3$ single crystals evaluated by scanning force microscopy. *Surf. Sci. Lett.* 2001, **480**, L402–L410.
14. Förderreuther, A., Thurn, G., Zimmermann, A. and Aldinger, F., R-curve effect, influence of electric field and process zone in $BaTiO_3$ ceramics. *J. Eur. Ceram. Soc.* 2002, **22**, 2023–2031.
15. Meschke, F., Raddatz, O., Kolleck, A. and Schneider, G. A., R-curve behaviour and crack-closure stresses in barium titanate and (Mg,Y)-PSZ ceramics. *J. Am. Ceram. Soc.* 2000, **83**, 353–361.
16. Howard, C. J. and Hunter, B. A., *A Computer Program for Rietveld Analysis of X-ray and Neutron Diffraction Patterns*. ANSTO Lucas Heights Research Laboratories, 1997.
17. Young, R. A., *The Rietveld Method, International Union of Crystallography*. Oxford University Press, 1993.
18. Kisi, E. H. and Howard, C. J., Elastic constants of tetragonal zirconia measured by a new powder diffraction technique. *J. Am. Ceram. Soc.* 1998, **81**, 1682–1684.
19. Ma, Y., Kisi, E. H. and Kennedy, S. J., Neutron diffraction study of ferroelasticity in a 3 mol%$Y_2O_3$–$ZrO_2$. *J. Am. Ceram. Soc.* 2001, **84**, 399–405.
20. Glazounov, A. E. and Hoffman, M. J., Investigation of domain switching in fractured ferroelectric ceramics by using imaging of X-ray diffraction. *J. Eur. Ceram. Soc.* 2001, **21**, 1417–1420.
21. Glazounov, A. E., Kungl, H., Reszat, J.-T., Hoffman, M. J., Kolleck, A., Schneider, G. A. *et al.*, Contribution from ferroelastic domain switching detected using X-ray diffraction to R-curves in lead zirconate titanate ceramics. *J. Am. Ceram. Soc.* 2001, **84**, 2921–2929.